

11-19-90  
E5704

NASA Technical Memorandum 103267

# A Study of Void Effects on the Interlaminar Shear Strength of Unidirectional Graphite Fiber Reinforced Composites

Kenneth J. Bowles and Stephen Frimpong  
*Lewis Research Center*  
*Cleveland, Ohio*

October 1990





A STUDY OF VOID EFFECTS ON THE INTERLAMINAR SHEAR STRENGTH  
OF UNIDIRECTIONAL GRAPHITE FIBER REINFORCED COMPOSITES

Kenneth J. Bowles and Stephen Frimpong  
National Aeronautics and Space Administration  
Lewis Research Center  
Cleveland, Ohio 44135

ABSTRACT

A study was conducted to evaluate the effect of voids on the interlaminar shear strength (ILSS) of a polyimide matrix composite system. The graphite/PMR-15 composite was chosen for study because of the extensive amount of experience that has been amassed in the processing of this material.

Composite densities and fiber contents of more than thirty different laminates were measured along with interlaminar shear strengths. Void contents were calculated and the void geometry and distribution were noted using microscopic techniques such as those used in metallography.

It was found that there was a good empirical correlation between ILSS and composite density. The most acceptable relationship between the ILSS and density was found to be a power equation which closely resembles theoretically derived expressions. An increase in scatter in the strength data was observed as the void content increased. In laminates with low void content, the voids appeared to be more segregated in one area of the laminate. It was found that void free composites could be processed in matched metal die molds at pressures greater than 1.4 MPa and less than 6.9 MPa.

INTRODUCTION

Fiber reinforced polymer matrix composites are now being used as production type materials of construction in the aircraft, aerospace and automotive industries. The successful use of these materials is based on the ability to exploit their high strength, high modulus and low density



characteristics. However, it is also contingent on the use of reproducible, economically feasible manufacturing techniques which produce structures satisfying the requirements established by the design engineer.

In general, for most fiber-resin systems, one of the component variables which is dependent on manufacturing techniques and curing procedures is void content. The void content, in turn, has a marked effect on composite interlaminar shear strength (ILSS) (Refs. 1 and 2) which has a significant effect on compressive strength, impact resistance and fatigue life (Refs. 3 to 5). The complete elimination of voids in composites produced by a full scale production facility may not be guaranteed for all fiber-resin systems and for this reason the effect of voids on the mechanical properties of composite materials must be considered, investigated and understood.

This paper describes the work that was directed toward the measurement of the effect of voids on the interlaminar shear strength of a polyimide matrix composite system. The Graphite/PMR-15 composite was chosen for study for the following reasons:

- (1) This system can be readily processed using the standard specified cure cycle to produce void free composites.

- (2) Preliminary work in this study has shown that the processing parameters of this resin matrix system can be altered to produce cured composites of varying void contents.

Thirty-eight 12-ply unidirectional composite panels were fabricated for this study. A significant range of void contents (0 to 10 percent) was produced. The panels were mapped, ultrasonically inspected (Ref. 6) and sectioned into interlaminar shear, flexure, and fiber content specimens. The density of each specimen was measured and interlaminar shear and flexure strength measurements were then made. The fiber content was measured last.



The results of these tests were evaluated using ultrasonic results (Refs. 6 and 7), photomicrographs, statistical methods, theoretical relationships derived by other investigators, and comparison of the test data with the Integrated Composite ANalyzer (ICAN) computer program that was developed at the NASA Lewis Research Center for predicting composite ply properties (Ref. 8). The testing program is described in as much detail as possible in order to aid in the accomplishment of realistic comparisons by others.

#### Experimental Procedures.

Monomeric reactant solution. - The monomers used in this study are shown in Table 1. The monomethylester of 5-norbornene-2,3 dicarboxylic acid (NE) and 4,4'-methylenedianiline (MDA) were obtained from commercial sources. The dimethylester of 3,3', 4,4'-benzophenonetetracarboxylic acid (BTDE) was synthesized as described in Ref. 9. Reactant solutions were prepared at a solids loading of 50 percent by weight in methanol. The stoichiometry of the reactants was adjusted to give a formulated molecular weight of 1500.

Composite fabrication. - Thirty-eight 12-ply unidirectional laminates were fabricated for this study. Each ply was cut from prepreg sheets that were made by drum-winding Hercules AS graphite fibers and impregnating the fibers with the PMR-15 monomer solution. Fiber tows with 10 000 fibers/tow were wound with a pitch of 3 tows/cm (7 tows/in.) The fiber was impregnated with an amount of monomer solution required to yield a cured ply thickness of 0.018 cm (0.08 in.) and a fiber content of about 60 wt % if no resin flow occurred. The prepreg was air dried for 1 hr on the drum. It was then heated to 49 °C (120 °F) on the drum for an additional hour. This drying procedure reduced the volatiles content to about 10 percent by weight. The result was a drapeable, nontacky prepreg.



After drying, the prepreg sheets were removed from the drum and cut into 7.62 cm (3 in.) by 25.40 cm (10 in.) plies with the fibers aligned with either the 25.40 cm (10 in.) direction (twenty-eight unidirectional laminates were fabricated with this orientation) or the 7.62 cm (3 in.) direction (eleven unidirectional laminates). For either orientation, twelve plies were stacked unidirectionally and imidized in a rectangular preforming cup for 3 hr at a temperature of 232 °C (450 °F) and an applied pressure of  $2.07 \times 10^{-3}$  MPa (0.3 psi). The final cure procedure involved heating a matched metal die mold to 232 °C (450 °F) and inserting the imidized preformed stack. The preform was contained in the die and held under press contact pressure for 10 min. After this initial dwell time, the cure pressure (which varied from specimen to specimen) was applied to the die and the mold temperature was increased to 315 °C (600 °F) at a rate of 5.5 °C (10 °F)/min. When a temperature of 316 °C (600 °F) was reached, the temperature and pressure were held for 1 hr. The cure pressures used in this study are presented in Fig. 1. These cure pressures produced a significant range of void contents and fiber/resin ratios. The properties of the fiber and the matrix materials are listed in Table 2.

The laminates were made in three groups. The groups were comprised of laminates 1 to 12, 20 to 30, and 31 to 48. Some laminates were discarded, so the number of laminates reported is 38 and not 42.

Specimen description. - Figure 2 is a mapping of a typical laminate that was fabricated with the fibers oriented in the longitudinal (25.4 cm (10 in.)) direction. These unidirectional panels are designated as panels 1 to 12 and 31 to 48. Panels 37, 43, and 45 were not tested.

Figure 3 depicts overall dimensions of the laminate panels designated as 20 to 30. The fiber orientation for these panels is in the transverse



(7.62 cm (3 in.)) direction. Both transverse and longitudinal fiber directions were used in this study to see if the path for resin flow during consolidation had any effect on mechanical properties reproducibility. A 1.59 cm (0.625 in.) wide strip was machined from each of the eleven panels that were made. These strips are designated as E strip in Fig. 3. The specimens that provided the data described herein for laminates 20 to 30 were machined from the E strips.

Ultrasonic scanning. - Before the 38 laminates were cut into test samples, they were mapped by two different ultrasonic procedures. Each laminate underwent a black-white C-scan and an amplitude scan. Typical results are shown in Fig. 4. The ultrasonic scan (Fig. 4(a)) shows variations in ultrasonic attenuation due to such factors as voids, delaminations, resin rich areas, etc. Areas of low attenuation show up as white areas in the scan and as low signal levels in the amplitude scans (Fig. 4(b)).

The scanning was done with the panels immersed in distilled water. They were positioned between two 2.5 MHz transducers - one sending and the other receiving. These laminates were subjected to a very extensive ultrasonic examination. In addition to the mapping, spot attenuation and velocity measurements were made using contact ultrasonics. Stress wave simulation measurements were made on each laminate. The ultrasonic evaluation of these specimens is described in detail elsewhere (Refs. 6 and 7).

Composite density. - Density measurements were made by a water immersion technique in accordance with ASTM D-792. The density measurement values and void contents are listed in Table 3 with the average standard deviations for all the 38 laminates and also for the three groups (1 to 12, 20 to 30 and 31 to 48). The standard deviations of these deviations are also tabulated in the same table for the 38 laminates and the three groups of laminates.



Fiber content. - The corresponding fiber volume fractions were calculated from the measured density data using the fiber and matrix densities. They can be compared with the spread of the actual fiber content data that was measured by acid digestion and presented in Table 4.

At least two short beam shear specimens from each of the 38 laminates were subjected to the  $H_2SO_4/H_2O_2$  digestion technique (ASTM D-3171) to measure the fiber content. The measured values are presented in Table 4, along with the differences between the two measurements. In addition one specimen from each of the laminates designated as 31 to 48 were sent to an independent testing laboratory for fiber content and void content measurement. These values are also listed in Table 4. The last two columns list the differences between the maximum and minimum measurements as a percentage of the average content from the sixth column of the table.

Void content. - The void content of each of the specimens was calculated from the measured fiber content and density measurement values. All values are presented in Fig. 1 and Table 3. The calculations were made using the following formula:

$$V_V = 1 - D_C(W_f/D_f + W_R/D_R)$$

$$V_V = \text{void volume fraction}$$

$$D_C = \text{measured composite density}$$

$$D_f = \text{fiber density} \quad (1)$$

$$D_R = \text{resin density}$$

$$W_f = \text{fiber weight fraction}$$

$$W_R = \text{resin weight fraction}$$

The value of the fiber density that was used was 1.799 g/cc (vendor's measurement). The value for the resin density was measured by water immersion (ASTM D-792) and was 1.313 g/cc. The reliability of the void content



determination is discussed in Ref. 10. The method is not accurate for void contents less than roughly 1 percent. For calculated void contents in this range, metallography was used as a tool to determine a reasonable estimate of the void content.

Metallography. - Three samples of the as-cured and untested material were taken from the L, P, and S areas of each E strip from laminates 20 to 30. The exception was 21 where samples were taken from the L and O areas. Metallographic samples were taken from the laminates designated 30 to 48 at the K, M, and P areas. The samples were mounted, polished and photographed at different magnifications, X30 to X160, to confirm the void size distribution and shape. Typical photomicrographs appear in Figs. 5 and 6. In addition, one or two of the short beam shear specimens from each group of samples representing the 39 different laminates were examined metallographically to determine the failure modes. In those cases where unusually high or low shear strength values were measured relative to the mean, two samples were examined. One sample was representative of the mean shear strength, and the other was the one that produced the unusual deviation.

Interlaminar shear strength. - All interlaminar shear tests were made at room temperature in accordance with ASTM D-2433 using a three point loading fixture with a constant span-to-depth ratio of 5. The rate of loading was 0.02 cm/sec (0.05 in./min). The number of specimens of each laminate that were tested varied from 8 to 20. Thickness varied from 0.23 to 0.25 cm (0.09 to 0.10 in.). These specimens were all 0.508 cm (0.2 in.) wide. The result of these tests are presented in Table 5.

Flexural strength. - The three point flexural tests were run in accordance with ASTM D-790 at a span/depth ratio of about 26. The width and



thickness were the same as those of the specimens used in the short beam shear tests. Twenty-two data points are presented in Table 6. Each point is the average of the data from six separate tests.

### Analysis of Results

Composite quality. - Figure 5 shows composite samples 35, 34, and 40 which contain 1.25, 3.9, and 12.1 percent voids, respectively. The specimens were sectioned perpendicular to the direction of the reinforcement. The voids are shown as holes between the fibers with those of Fig. 5(c) being circular in shape. In Fig. 6, the same specimens are shown but with the sectioning oriented parallel to the reinforcement direction. In this view, the voids are shown as long slits. From the information presented by these two figures, it appears that the voids are more or less cylindrical in shape, and situated between the plies. The specimens with the low void contents do not have the voids evenly distributed throughout the volume of the composites. In the case of specimen 35 (1.25 percent voids) the voids are not evenly distributed among the ply interfaces, but apparently segregated at one portion of the composite cross section. The void fractions are estimated from the voids in Fig. 5, by measurement of the relative lengths of voids to matrix. They comprise 44, 22, and 36 percent of the interlaminar matrix material. It does appear that the void distribution may become more homogeneous as the void content increases (Fig. 5(c)). In considering the low void content composites, one can infer that the interlaminar shear strength of the composite is dependent on the location of the voids. If they are located near the outer surfaces, there should be no effect on the shear strength since theoretically, the shear stresses increase from zero at the specimen surfaces to a maximum at the neutral plane. If they are located near the inner high shear stress areas then they can cause premature failure (lower calculated failure stresses).



As previously indicated, the details of the ultrasonic examinations of the specimens are presented in detail elsewhere (Refs. 6 and 7). It was found that an ultrasonic-acoustic technique utilizing the measurement of the stress wave factor, was effective in evaluating the interlaminar shear strength of fiber reinforced composites. The details of this portion of the study can be obtained from these references.

Composited densities and fiber content. - Composite densities and fiber volume fractions are presented in Table 3. The density value that is listed for each of the 38 specimens is the numerical average calculated for the number of specimens listed in the table for each of the three groups of specimens. A total of 403 density measurements were made. The mean and standard deviation were calculated for each group of specimens and then the mean and standard deviation of the 38 values from the laminates were also calculated and are included in the table. All laminates except 5, 36, and 40 had measured densities with standard deviations less than 1 percent. The corresponding changes in fiber volume fractions were calculated using the following relationship:

$$\Delta V_f = \Delta D_C(1-V_v)/0.486 \quad (2)$$

$\Delta V_f$  = The change in fiber volume fraction.

$\Delta D_C$  = The change in composite density.

Actual differences between composite fiber volume fraction differences for each laminate are also shown in Table 3. They have been calculated as the difference between the maximum and minimum fiber volume fraction values for each group of specimens that were digested. The measured fiber volume fractions are the values that are presented in Table 4. The majority of the measurements were made at NASA Lewis but a series of digestions were also performed at a commercial laboratory and are also listed in the table. The



standard deviations of the differences between the values measured at NASA Lewis and those measured at the private laboratory are also tabulated in Table 4. The calculated standard deviations for these values, that were measured by the digestion method, are about 2.5 times the values converted to fiber volume fractions by calculations using the density data. The average difference was about 3 percent. The number of specimens that were digested was 64. There appear to be no trends in the data in Table 3 as indicated by the average standard deviations of the three groups or in Table 4. The average standard deviation of the density measurements in Table 3 is 0.58 percent while the standard deviation of the fiber content, as measured by acid digestion (Table 4), is 2.23 percent. It is evident that the density measurements by water immersion produce more consistent results than density measurements calculated from fiber fraction content data measured by the acid digestion procedure. The digestion measurements are necessary for calculating the void contents.

Void content. - In spite of the variations in the fiber content measurements shown in Table 4, the calculated void contents in Table 3 show very good agreement within each group of specimens. Except for specimen 36, they all appear to be within a percent of each other.

The cure pressure for each laminate is included in Fig. 1 and, at each end of the pressure spectrum that was investigated, the void content increases. At the low end [ $<1.4$  MPa (200 psi)], the voids increase, probably because of the lack of pressure needed to sweep out the volatiles and air pockets within the fluidized matrix. Apparently when the higher pressures are applied [ $>6.9$  MPa (1000 psi)], there may be a trapping of the volatiles and air within the laminate, resulting in void formation. When the cure pressures are held between 5.5 MPa (800) and 1.4 MPa (200 psi), it appears that void free laminates are produced. There does not seem to be a clear indication of



differences in void content due to fiber orientation ( $0^\circ$  or  $90^\circ$ ) or on mechanical properties variations within a group of laminates cured under the same pressure for this size of specimens.

Interlaminar shear strength. - Table 5 contains the data from the 409 individual short beam shear tests from the 38 groups of specimens. Standard deviations of each of the groups are presented in both MPa (ksi) and percent of the average ILSS value along with the average standard deviation and the standard deviation of the standard deviations of the 38 laminates. The standard deviation for the whole group is 4.7 percent. For a 99.9 percent confidence factor, the ILSS values are grouped within a  $\pm 7.5$  percent band as determined by the  $3\sigma$ . The values that are outside this limit are those for the specimens numbered 31, 36, 39, and 40. Examination of Fig. 1 and Tables 3 and 4 does not reveal a trend for such behavior. For the purposes of this report, the specimens were divided into three groups corresponding to their time of fabrication and testing. The first group (1 to 12) contains only void-free composites. The second group (20 to 30) includes laminates with void contents from 0 to 6 percent. The third group contains laminates with void contents from 6 to 10 percent. It can be seen that as the void content increases, the average standard deviation increases with increasing void content from 3.7 to 4.1 percent and then to 8.1 percent. The large standard deviations in the ILSS measurements, as compared to the standard deviations of the density measurements, are due to random defects in the composites (such as voids) that at times are positioned so that they cause premature failure. As previously discussed, the distribution of defects is illustrated by microscopic examination, as shown in Figs. 5 and 6. Although the void content of specimen 40 is 10 percent, these voids are distributed evenly through the sample.



Specimen 36, with a void content of 8.1 percent, has the voids segregated primarily between the plies.

Specimens 31 to 39 were examined microscopically after they were tested to locate the position at which the shear failures occurred. The estimate of the failure positions varied from 1/4 to 1/3 to 1/2 the distance from one surface to the other surface. It cannot be guaranteed that the observed failures are those that actually initiated the specimen failures. They may be secondary in nature. Theoretically short beam shear failures occur at the midplane. The possible segregation of the voids at the ply interfaces may cause failure away from the midplane. No correlation could be found between the observed failure position and the shear strength. It is highly unlikely that a study such as this will be successful because of the necessity for pinpointing the defect or position at which the initiation of failure occurred.

ILSS correlation with void and fiber content. - If one examines Fig. 7, it is apparent that there is a good correlation between the composite ILSS and composite density. The scatter is greatest at the low density end of the plot. This relationship is shown in both a linear and power equation configuration in the figure. These relationships are well-suited since the data indicate that the composite density measurements are more consistent than the fiber fraction data from acid digestion. The measured ILSS data were fitted to the two types of equations with composite density as the dependent variable. The density is expressed in terms of the fiber and void fractions in order to allow comparison of the equations with those equations that exist in the literature (Ref. 11). The relationship that is used is:

$$D_C = (1 - V_V)(0.486V_f + 1.33) \quad (3)$$

The consensus of opinion is that there are two possible configurations for voids in composites. The two possibilities are cylindrical and spherical.



The equations that were theoretically derived for cylindrical and spherical voids and published in Ref. 11 are:

$$\text{Cylindrical.} \quad \text{ILSS}_r = [1 - (4V_v/3.14(1 - V_{fv}))]^{1/2} \quad (4)$$

$$\text{Spherical.} \quad \text{ILSS}_r = (1 - 3.1416/4[6V_v/3.1416(1 - V_{fv}))]^{2/3} \quad (5)$$

$V_{fv}$  is the fiber volume fraction of the composite with voids.

$\text{ILSS}_r$  is the relative ILSS of the composite with voids to that of the void free composite ILSS.

The power equation produced the best fit in respect to the calculated correlation coefficients. The  $R^2$  values were 0.45 and 0.86 for the linear and power regressions, respectively. When only those data points from specimens that contained no voids were analyzed, the  $R^2$  value for the linear equation fit increased to 0.593. The linear and power relationships between ILSS and composite density are as follows:

$$\text{ILSS (MPa)} = 15.907(1 - V_v)(0.486V_f + 1.313)^{-2.708} \quad (6)$$

$$\text{ILSS (MPa)} = 14.031(1 - V_v)(0.486V_f + 1.313)^{4.46} \quad (7)$$

Equation 7 was used to generate the sensitivity analyses displayed in Table 7. Equation 7 was selected to represent the measured values because it has a much better  $R^2$  value than Eq. 6 and mathematically, it is similar to the theoretically derived Eqs. 4 and 5. However, Eq. 6 can be used to quickly calculate a reasonable value for the ILSS of a composite with a known density. Tables 8 and 9 contain sensitivity analyses calculated using Eqs. 4 and 5 for composites with cylindrical and spherical voids. The values are calculated as percent of the void-free laminate ILSS ( $\text{ILSS}_r$ ).

The sensitivity analysis in Table 7 indicates that there is about an 11 percent decrease in composite ILSS for a 10 percent decrease in fiber content from 60 to 50 percent. An 11 percent increase in void content is



reflected as a 40 percent drop in composite ILSS. The models presented in Tables 8 and 9 show a larger effect from fiber content changes on the ILSS and a significantly greater effect from void content changes.

The data for four different types of composites with 0.6 fiber volume fraction are plotted in Fig. 8. The types of composites are as follows:

- (1) Measured data
- (2) Spherical void content
- (3) Cylindrical void content
- (4) Composite modeled by ICAN (Ref. 8)

It is evident that the measured data from this study closely approximates the curve produced with values calculated using the relationship between ILSS and spherical void content. The models suggest that cylindrical voids would produce lower values of ILSS. The very close correlation between the measured data and the curve for a composite with spherical voids does not support the metallographic evidence observed in Figs. 5 and 6 which led to the conclusion that the voids in the laminates that were studied were cylindrical in shape. The equation incorporated in the ICAN program is similar to that for cylindrical voids in Ref. 11. The curves shown for these two relationships (numbers 3 and 4) do lie close together. The ILSS data from this study indicate that the voids act as spherical voids in reducing the ILSS. This significant inconsistency can only be explained by conjecture. It may be that the voids can be considered as small delaminations or cracks or of some other configuration which can be modeled and gives the same type of equation as the spherical void model.

From the results of this study, the ICAN program can be improved for the laminates described herein by assuming spherical void behavior rather than the current cylindrical void relationship. In addition to the correction for void



shape, it was found that the ICAN predicted values for the ILSS for the composite material studied in this program were almost one-half the measured values. Attempts by other investigators to calculate the shear strength have been unsuccessful (1). Measured values of composite shear strengths have been found to exceed the shear strength of the matrix. Examination and comparison of the ILSS data predicted by ICAN that is shown in Table 10 with the data in Tables 2 and 5 show this. It would seem necessary to include a factor for the degree of interfacial bonding between the fiber and the matrix or to confirm the matrix and fiber shear properties in any model derived for predicting the ILSS of polymer matrix composite materials.

Flexural strength. - The flexural strengths of specimens from some of the laminates are plotted as a function of the corresponding ILSS in Fig. 9. There appears to be a relationship between the two mechanical properties. The  $R^2$  value is a relatively low value of 0.786. Similar relationships are reported for boron and graphite fiber reinforced composites in Ref. 12.

The nonlinearity of the relationship is more obvious from the data from this study and can be clarified by plotting the data from this study as is shown in Fig. 10. The curves in both Figs. 9 and 10 are similar, indicating the possibility that the nonlinearity is due to the variation in fiber content. It is proposed that for the composites with higher fiber content (higher density) the flexural failure is due to a tensile failure on the side opposite the load point. The superimposed upper dashed line in Fig. 10 is a plot of the slope of the relationship for tensile flexural strength of a composite as a function of fiber content. Likewise the lower dashed line is a plot of the slope of the compressive flexural failure strength as a function of fiber content. The modeled failure mechanism is delamination. Both



equations were taken from Ref. 8. For the specimens studied in this work, the information presented in Fig. 10 indicates the possibility that the nonlinear relationship may be attributed to changing failure mechanisms. As the voids increase and the ILSS decreases, the mechanism changes from that of a tensile failure to that of a compressive failure. In Ref. 12 plots of composite compressive strength as a function of ILSS show exactly the same behavior. The lower ILSS results in a decrease in the compressive strength.

Summary. - An extensive study was conducted to relate the interlaminar shear strength of AS4/PMR-15 unidirectional composites with both fiber and void contents. Composite densities and fiber contents were measured along with the interlaminar shear strengths of 39 different composite laminates. Void contents were calculated and the void geometry and distribution were noted using microscopic examination techniques such as those used in metallography. The measured data were fitted to various types of curves using regression analyses. It was found that there were good empirical correlations between strength and composite density.

The most logical relationship between ILSS and density seems to be the power equation (Eq. 7). This is based on the close resemblance to the theoretically derived equations from Ref. 10 and the relatively good fit of the data. From comparison of the data calculated using Eq. 7 with those from Eqs. 4 and 5, it was found that a very good correlation exists between the empirically derived relationship from this study and the ILSS values predicted by the spherical void model. High magnification photographs of polished surfaces indicated that the majority of voids were in the form of cylinders. The ICAN program that was developed at NASA Lewis predicts a relationship based on cylindrical voids and thus predicts lower ILSS values than the measured ones. No model was found that accurately predicts the absolute value of ILSS for the AS4/PMR-15 composite.



It was found that there was more scatter in the composite strength values as the void content increased. Composite fiber content calculated from density measurements were more consistent than those measured by the acid digestion technique. It appears that the distribution of voids within the composites became more homogeneous as the void content increased. In those laminates with low void content, the voids appeared to be more segregated in one area of the laminate.

The results of this study indicate that void free composites can be processed at pressures greater than 1.4 MPa (200 psi) and less than 5.5 MPa (1000 psi).



## REFERENCES

1. Hancox, N.L., "The Effects of Flaws and Voids on the Shear Properties of CFRP," J. Mater. Sci., 12: 884-892 (1977).
2. Yoshida, H., Ogasa, T., Hayashi, R., "Statistical Approach to the Relationship Between ILSS and Void Content of CFRP," Compos. Sci. Technol., 25: 3-18 (1986).
3. Kunz, S.C. and Beaumont, P.W.R., "Microcrack Growth in Graphite Fiber-Epoxy Resin Systems During Compressive Fatigue," Fatigue of Filamentary Composite Materials; Proceedings of the Symposium. ASTM STP 569 American Soc. for Testing and Materials, 71-91 (1975).
4. Greszczuk, L.B., "Compressive Strength and Failure Modes of Unidirectional Composites, Analysis of the Test Methods for High Modulus Fibers and Composites; Proceedings of the Symposium." ASTM-STP 521, American Soc. for Testing and Materials, 192-217 (1973).
5. Bowles, K.J., "The Correlation of Low Velocity Impact Resistance of Graphite-Fiber-Reinforced Composites With Matrix Properties," Composite Materials: Testing and Design. T.D. Whitcomb, ed., ASTM-STP 972, American Soc. for Testing and Materials, 124-142 (1988).
6. Vary, A. and Bowles, K.J., Ultrasonic Evaluation of the Strength of Unidirectional Graphite-Polyimide Composites. NASA TM X-73646 (1977).
7. Vary, A. and Bowles, K.J., "An Ultrasonic-Acoustic Technique for Nondestructive Evaluation of Fiber Composite Quality," Polymer Eng. Sci., 19: 373-376 (April 1979).
8. Murthy, P.L.N. and Chamis, C. Integrated Composites Analyzer (ICAN): Users and Programmers Manual NASA TP-2515 (1986).



9. Serafini, T.T. and Vannucci, R.D., "Tailor Making High Performance Graphite Fiber Reinforced PMR Polyimides," Presented at the Thirtieth Annual Reinforced Plastics Composites Conference sponsored by the Society of the Plastics Industry, Feb. 4-7, 1975 (Also, NASA TM-X-71616, 1974).
10. Cilley, E., Roylance, D., and Schneider, N., "Methods of Fiber and Void Measurement in Graphite/Epoxy Composites," Composite Materials: Testing and Design; Proceedings of Third Conference ASTM STP 546, American Soc. for Testing and Materials, 237-249 (1974).
11. Greszczuk, L.B., "Effect of Voids on Strength Properties of Filamentary Composites", International Reinforced Plastics Division Annual Technical Conference 22nd Proceedings. New York: Soc. of the Plastics Industry, 20-A.1-20-A.10 (1967).
12. Petker, I., "The Status of Organic Matrices in Advanced Composites, A Personalized View" SAMPE Q., 3: 7-21 (1972).



TABLE 1. - MONOMERS USED FOR PMR-15 POLYIMIDE

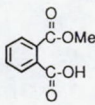
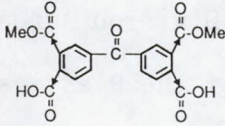
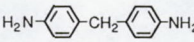
Structure	Name	Abbreviation
	Monomethyl Ester of 5-Norbornene-2,3-Dicarboxylic acid	NE
	Dimethyl ester of 3,3',4,4'-Benzophenonetetracarboxylic acid	BTDE
	4,4'-Methylenedianiline	MDA

TABLE 2. - CONSTITUENT PROPERTIES<sup>a</sup>

Property	As graphite	PMR-15 matrix
Logitudinal tensile modulus, GPa (Msi)	213.7(31)	3.2(0.470)
Transverse tensile modulus, GPa (Msi)	13.7(2)	
Shear modulus 12, GPa (Msi)	13.7(2)	1.1(0.173)
Shear modulus 23, GPa (Msi)	6.8(1)	
Poisson's ratio	0.3	0.36
Tensile strength, MPa (ksi)	3033.8(440)	55.8(8.1)
Compression strength, MPa (ksi)	-----	11.37(16.5)
Shear strength, MPa, (ksi)	-----	55.8(8.1)
Density, g/cm <sup>3</sup>	1.799	1.313

<sup>a</sup>Reference 11.



TABLE 3. - DENSITY OF COMPOSITES

Specimen number	Number of samples	Density, g/cm <sup>3</sup>	Standard deviation		Calculation deviation in fiber fraction percent	Measured deviation of fiber fraction, percent
			g/cm <sup>3</sup>	Percent		
1	1.595	8	10.5x10 <sup>3</sup>	0.66	1.35	7.48
2	1.587		2.9	.18	.38	.04
3	1.575		5.5	.35	.72	1.17
4	1.613		8.4	.52	1.07	1.11
5	1.521		18.9	1.24	2.55	2.08
6	1.622		11.3	.70	1.43	1.51
7	1.566		13.8	.88	1.81	15.57
8	1.573		8.0	.51	1.05	.12
9	1.596		5.5	.34	.71	4.99
10	1.581		8.0	.51	1.04	1.76
11	1.583		13.5	.85	1.75	6.42
12	1.623	12	13.5	.83	1.71	3.27
20	1.581	8	5.5	.35	.72	.05
21	1.569	20	15.2	.97	1.97	.38
22	1.552	18	10.0	.64	1.31	2.10
23	1.558	20	4.7	.30	.61	7.99
24	1.517	20	5.3	.35	.69	4.09
25	1.573	20	13.9	.88	1.82	1.51
26	1.500	10	5.9	.39	.77	.64
27	1.477	20	5.1	.35	.67	6.01
28	1.529	19	9.5	.62	1.25	5.30
29	1.510	20	7.4	.49	.97	1.57
30	1.575	8	5.5	.35	.72	1.07
31	1.568	8	8.2	.52	1.08	2.78
32	1.561	6	4.1	.26	.54	1.01
33	1.570	8	4.5	.29	.59	.91
34	1.515		10.0	.66	1.31	2.92
35	1.539		6.2	.40	.82	1.53
36	1.461		22.9	1.57	2.97	1.00
38	1.443		5.7	.40	.75	4.07
39	1.456		11.9	.82	1.57	1.32
40	1.356		24.8	1.83	3.31	.68
41	1.453		10.4	.72	1.36	2.68
42	1.417		7.4	.52	.98	3.37
44	1.561		4.2	.27	.55	5.07
46	1.574		5.4	.34	.71	4.93
47	1.464		4.2	.29	.55	4.91
48	1.469		5.4	.37	.71	2.70

Total average standard deviation	0.59
Total standard deviation	0.35
Specimens 1 to 12:	
Average standard deviation	0.63
Standard deviation	0.28
Specimens 20 to 30:	
Average standard deviation	0.52
Standard deviation	0.22
Specimens 31 to 48:	
Average standard deviation	0.62
Standard deviation	0.46



TABLE 4. - FIBER CONTENT MEASUREMENTS BY ACID DIGESTION TECHNIQUES

Specimen number	Lewis fiber measurement				Independent testing laboratory		
	Measurement, percent			Average, percent	Difference (max. to min.), percent	Measurement, percent	Lewis average - independent measurement, percent
	1	2	3				
1	53.49	58.13	-----	56.04	4.19	-----	-----
2	54.23	54.25	-----	54.24	.02	-----	-----
3	54.38	53.75	-----	54.07	.63	-----	-----
4	57.88	57.24	-----	57.56	.64	-----	-----
5	49.41	50.45	-----	49.93	1.04	-----	-----
6	59.93	60.84	-----	60.39	.91	-----	-----
7	54.49	46.62	-----	50.56	7.87	-----	-----
8	51.71	51.77	-----	51.74	.06	-----	-----
9	57.28	54.49	-----	55.89	2.79	-----	-----
10	53.09	54.03	-----	53.56	.94	-----	-----
11	51.25	54.65	-----	52.95	3.40	-----	-----
12	62.79	60.77	-----	61.78	2.02	-----	-----
19	55.92	55.90	56.17	55.30	.48	-----	-----
21	58.38	58.64	56.28	57.77	4.02	-----	-----
22	54.85	53.71	54.08	54.21	2.08	-----	-----
23	55.49	55.94	51.58	54.34	7.79	-----	-----
24	59.66	57.26	58.12	58.35	4.13	-----	-----
25	57.77	58.64	57.99	57.99	1.48	-----	-----
26	55.29	55.49	55.14	55.31	.63	-----	-----
27	56.38	53.09	53.90	54.46	5.84	-----	-----
28	54.63	53.68	51.77	53.36	5.24	-----	-----
29	55.83	58.03	54.96	56.27	5.29	-----	-----
30	55.36	55.15	55.74	55.42	1.06	-----	-----
31	51.29	52.74	-----	52.02	1.45	52.20	-0.19
32	50.57	51.08	-----	50.83	.51	50.00	.83
33	52.38	52.86	-----	52.62	.48	53.80	-1.18
34	50.10	51.59	-----	50.85	1.49	51.19	-.34
35	51.36	50.58	-----	50.97	.78	50.63	.34
36	48.75	48.27	-----	48.51	.48	46.89	1.62
38	46.23	48.16	-----	47.20	1.93	47.70	-.50
39	48.31	48.95	-----	48.63	.64	48.42	.21
40	43.67	43.96	-----	43.82	.29	41.47	2.64
41	47.35	48.64	-----	48.00	1.29	48.60	-.61
42	44.50	46.03	-----	45.27	1.53	45.79	-.52
44	48.61	51.71	-----	49.89	2.56	51.60	-1.71
46	51.76	54.40	-----	53.08	2.64	54.60	-1.52
47	46.42	48.78	-----	47.60	2.36	48.97	-1.37
48	47.87	49.19	-----	48.53	1.32	49.37	-.84

	Lewis difference (max. to min.), percent	Lewis average-independent measurement, percent
Average standard deviation	2.17	-0.21
Standard deviation	2.02	1.16
Specimens 1 to 12:		
Average standard deviation	2.04	-----
Standard deviation	2.17	-----
Specimens 19 to 30:	3.46	-----
Average standard deviation	2.34	-----
Standard deviation		
Specimens 31 to 48:	1.32	-----
Average standard deviation	.76	-----
Standard deviation		



TABLE 5. - ROOM TEMPERATURE ILSS DATA FOR UNIDIRECTIONAL COMPOSITES

Specimen number	Number of samples	ILSS		Standard deviation		
		MPa	ksi	MPa	psi	Percent
1	8	122.0	17.7	6.0	$8.7 \times 10^{-2}$	4.92
2		108.9	15.8	1.9	2.8	1.77
3		111.0	16.1	4.6	6.7	4.16
4		108.9	15.8	2.8	4.0	2.53
5		91.0	13.2	3.2	4.6	3.48
6		113.8	16.5	3.7	5.4	3.27
7		104.8	15.2	3.6	5.2	3.42
8		108.3	15.7	3.3	4.8	3.06
9	9	112.4	16.3	5.2	7.6	4.66
10	10	108.3	15.7	4.5	6.5	4.14
11	11	110.3	16.0	4.4	6.4	4.00
12	12	124.8	18.1	6.0	8.7	4.81
19	8	113.8	16.5	4.9	7.1	4.30
21	20	111.7	16.2	5.2	7.5	4.63
22	18	97.3	14.2	3.7	5.3	3.73
23	20	102.7	14.9	4.2	6.1	4.09
24	20	90.3	13.1	2.4	3.5	2.67
25	20	114.5	16.6	3.4	4.9	2.95
26	10	83.4	12.1	3.2	4.6	3.80
27	20	80.7	11.7	2.1	3.1	2.65
28	19	97.2	14.1	9.9	14.4	10.21
29	20	89.6	13.0	3.2	4.6	3.54
30	8	107.6	15.6	3.0	4.4	2.82
31		94.5	13.7	12.5	18.1	13.21
32		105.5	15.3	4.0	5.8	3.79
33		107.6	15.6	3.6	5.2	3.33
34		90.3	13.1	4.7	6.8	5.19
35		101.4	14.7	3.2	4.7	3.20
36		66.2	9.6	6.1	8.9	9.27
38		61.4	8.9	3.6	5.2	5.84
39		64.8	9.4	6.5	9.4	10.00
40		66.9	9.7	7.6	11.0	11.34
41		66.2	9.6	3.4	4.9	5.10
42		77.9	11.3	2.8	4.1	3.63
44		106.2	15.4	3.6	5.2	3.38
46		103.4	15.0	5.9	8.5	5.67
47		73.8	10.7	5.9	8.5	7.94
48		75.8	11.0	3.9	5.6	5.09

	Standard deviation		
	MPa	psi	Percent
Total average standard deviation	4.5	$6.5 \times 10^{-2}$	4.88
Total standard deviation	2.1	3.1	2.60
Specimens 1 to 12:			
Average standard deviation	----	-----	3.70
Standard deviation	----	-----	.91
Specimens 19 to 30:			
Average standard deviation	----	-----	4.13
Standard deviation	----	-----	2.03
Specimens 31 to 48:			
Average standard deviation	----	-----	8.12
Standard deviation	----	-----	3.09



TABLE 6. - ROOM TEMPERATURE FLEXURAL STRENGTH OF COMPOSITES

Specimen number	Number of tests	Average flexural strength		Standard deviation			
		MPa	ksi	MPa	ksi	Percent	
1	6	1838.9	266.7	41.4	6.0	2.25	
2	6	1704.4	247.2	67.6	9.8	3.96	
3	6	1627.2	236.0	114.5	16.6	7.03	
4	4	1860.3	269.8	75.2	10.9	4.04	
5	6	1506.6	218.5	95.2	13.8	6.32	
6	4	1972.7	286.1	82.1	11.9	4.16	
7	6	1666.5	241.7	46.9	6.8	2.81	
8	6	1573.4	228.2	83.4	12.1	5.30	
9	5	1701.7	246.8	113.1	16.4	6.65	
10	4	1860.3	269.8	75.2	10.9	4.04	
11	6	1762.4	255.6	72.4	10.5	4.11	
12	6	1997.5	289.7	72.4	10.5	3.62	
31	6	1361.1	197.4	91.0	13.2	6.69	
32	4	1290.1	187.1	100.7	14.6	7.80	
33	2	1474.2	213.8	20.7	3.0	1.40	
34	3	1108.0	160.7	63.4	9.2	5.72	
35	8	1230.8	178.5	38.6	5.6	3.14	
39	8	932.2	135.2	162.0	23.5	17.38	
40	9	925.3	134.2	58.6	8.5	6.33	
41	10	1059.1	153.6	63.4	9.2	5.99	
42	9	1143.9	165.9	46.9	6.8	4.10	
44	4	1496.2	217.0	53.8	7.8	3.59	
46	8	1588.6	230.4	49.6	7.2	3.13	
47	9	1178.4	170.9	89.6	13.0	7.61	
48	3	1136.3	164.8	35.9	5.2	3.16	
		Average standard deviation					5.21
		Standard deviation					3.01

TABLE 7. - SENSITIVITY ANALYSIS OF ILSS FOR COMPOSITES  
WITH VOIDS AND FIBER CONTENT AS VARIABLES (EQ. 7)

Void volume, $V_v$ , percent	Fiber volume, $V_f$ , percent										
	60	59	58	57	56	55	54	53	52	51	50
	Percent of initial ILSS										
0	100	99	97	96	95	93	92	91	90	88	87
1	96	94	93	92	91	89	88	87	86	85	83
2	91	90	89	88	87	85	84	83	82	81	80
3	87	86	85	84	83	82	80	79	78	77	76
4	83	82	81	80	79	78	77	76	75	74	73
5	80	78	77	76	75	74	73	72	71	70	69
6	76	75	74	73	72	71	70	69	68	67	66
7	72	71	70	69	69	68	67	66	65	64	63
8	69	68	67	66	65	64	64	63	62	61	60
9	66	65	64	63	62	61	61	60	59	58	57
10	63	62	61	60	59	58	58	57	56	55	54
11	59	59	58	57	56	56	55	54	53	53	52



TABLE 8. - CYLINDRICAL VOID MODEL SENSITIVITY ANALYSIS OF ILSS AS FUNCTION OF FIBER AND VOID CONTENT

Void volume, $V_v$ , percent	Fiber volume, $V_f$ , percent										
	60	59	58	57	56	55	54	53	52	51	50
	Percent of initial ILSS										
0	100.0000	100.0000	100.0000	100.0000	100.0000	100.0000	100.0000	100.0000	100.0000	100.0000	100.0000
1	82.2898	82.5019	82.7066	82.9042	83.0952	83.2800	83.4588	83.6320	83.7999	83.9627	84.1207
2	75.1318	75.4226	75.7035	75.9750	76.2376	76.4917	76.7379	76.9765	77.2079	77.4324	77.6505
3	69.7518	70.0975	70.4316	70.7548	71.0676	71.3705	71.6642	71.9490	72.2253	72.4937	72.7544
4	65.3044	65.6920	66.0670	66.4299	66.7815	67.1222	67.4526	67.7733	68.0847	68.3872	68.6813
5	61.4586	61.8798	62.2875	62.6824	63.0652	63.4364	63.7966	64.1464	64.4863	64.8166	65.1380
6	58.0430	58.4918	58.9264	59.3477	59.7563	60.1528	60.5378	60.9118	61.2755	61.6291	61.9733
7	54.9550	55.4267	55.8839	56.3273	56.7575	57.1754	57.5813	57.9759	58.3597	58.7331	59.0967
8	52.1270	52.6180	53.0942	53.5564	54.0051	54.4411	54.8649	55.2771	55.6782	56.0687	56.4491
9	49.5117	50.0191	50.5115	50.9897	51.4543	51.9059	52.3451	52.7725	53.1886	53.5939	53.9889
10	47.0744	47.5958	48.1022	48.5941	49.0723	49.5374	49.9900	50.4306	50.8598	51.2780	51.6857

TABLE 9. - SPHERICAL VOID MODEL SENSITIVITY ANALYSIS OF ILSS AS FUNCTION OF FIBER AND VOID CONTENT

Void volume, $V_v$ , percent	Fiber volume, $V_f$ , percent										
	60	59	58	57	56	55	54	53	52	51	50
	Percent of initial ILSS										
0	100.0000	100.0000	100.0000	100.0000	100.0000	100.0000	100.0000	100.0000	100.0000	100.0000	100.0000
1	92.0682	91.9787	91.8868	91.7921	91.6946	91.5942	91.4907	91.3839	91.2738	91.1600	91.0425
2	87.3231	87.1801	87.0331	86.8818	86.7261	86.5656	86.4001	86.2295	86.0534	85.8716	85.6838
3	83.2778	83.0893	82.8954	82.6958	82.4903	82.2786	82.0604	81.8353	81.6030	81.3632	81.1154
4	79.6096	79.3797	79.1432	78.8999	78.6493	78.3912	78.1251	77.8506	77.5674	77.2750	76.9728
5	76.1857	75.9172	75.6411	75.3569	75.0642	74.7627	74.4520	74.1314	73.8007	73.4591	73.1062
6	72.9357	72.6306	72.3167	71.9937	71.6611	71.3185	70.9653	70.6010	70.2251	69.8370	69.4359
7	69.8164	69.4762	69.1261	68.7659	68.3950	68.0128	67.6190	67.2127	66.7935	66.3606	65.9133
8	66.7994	66.4251	66.0401	65.6439	65.2359	64.8155	64.3823	63.9354	63.4743	62.9981	62.5062
9	63.8645	63.4571	63.0380	62.6068	62.1627	61.7052	61.2337	60.7473	60.2454	59.7272	59.1917
10	60.9968	60.5571	60.1048	59.6393	59.1600	58.6662	58.1572	57.6323	57.0906	56.5312	55.9532

TABLE 10. - ROOM TEMPERATURE  
ILSS OF COMPOSITES WITH  
DIFFERENT VOID  
FRACTIONS

Percent voids	ILSS	
	MPa	ksi
0	57.9	8.4
1	47.6	6.9
2	42.7	6.2
4	35.8	5.2
6	30.3	4.4
8	24.8	3.6
10	20.0	2.9



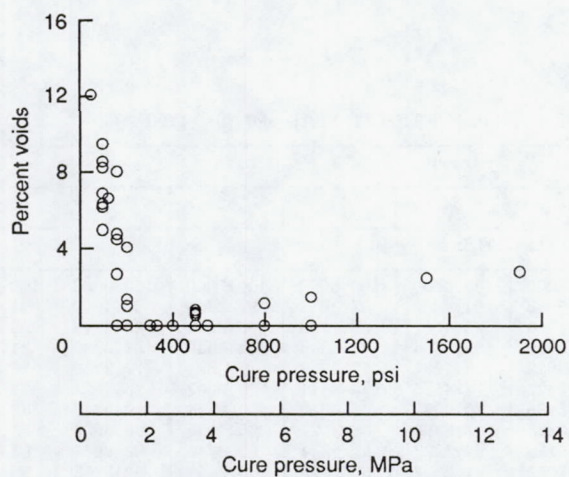


Figure 1.—Composite void content as a function of cure pressure.

Specimen excision schematic for longitudinal series (1-12 and 31-48)

Code:

F = Flexure

I = Impact

T = Tensile

SB = Short beam shear

J thru Q Spare SB  
R thru Y Density and micros

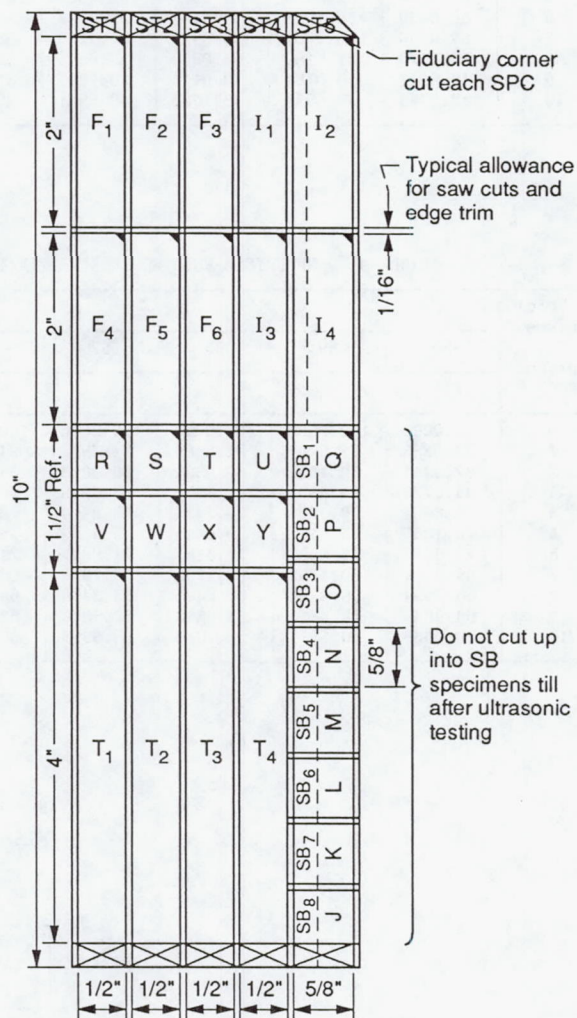


Figure 2.—Longitudinal laminate schematic.



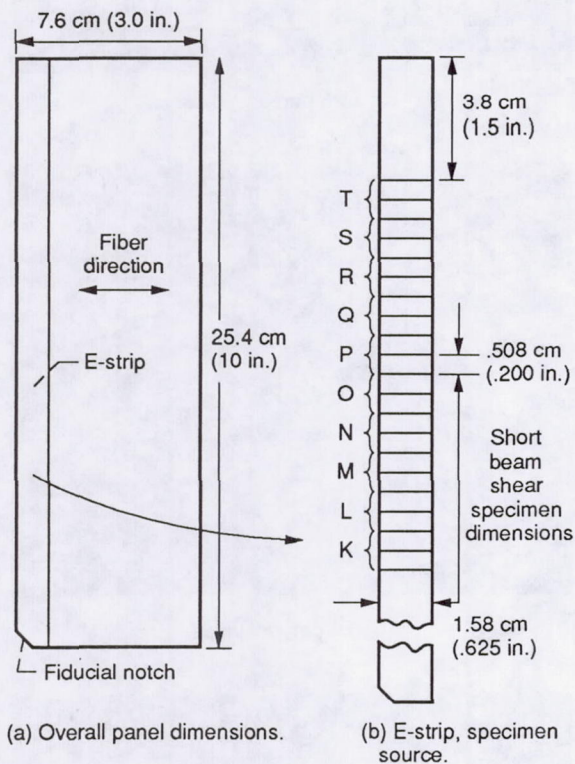
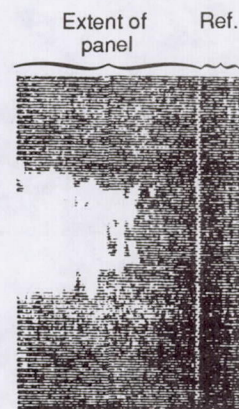
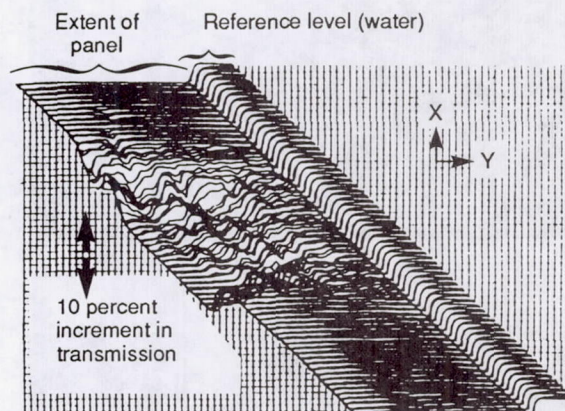


Figure 3.—Transverse laminate schematic.



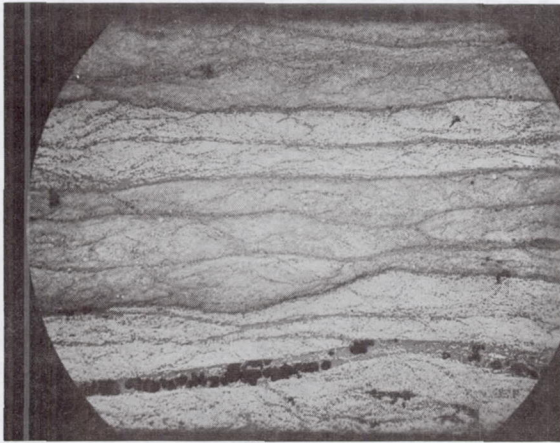
(a) Example of a conventional ultrasonic black-white C-scan.



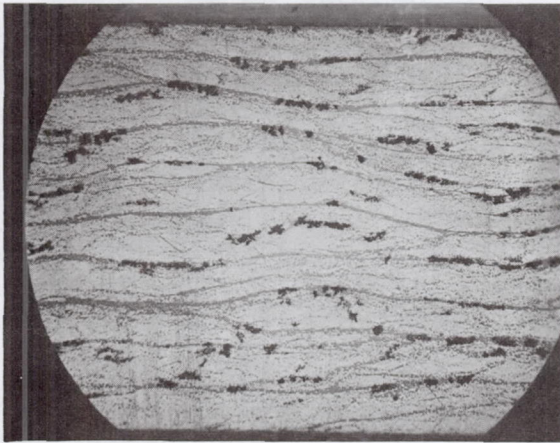
(b) Example of amplitude scan of same object as that in Figure 2(a). Object is a flat composite panel selected to show a range in ultrasonic transmission.

Figure 4.—Illustration of various through-transmission ultrasonic scan images indicating variation of transmitted ultrasound due to attenuation by voids and fiber fraction variations in typical graphite-polyimide composite panels.

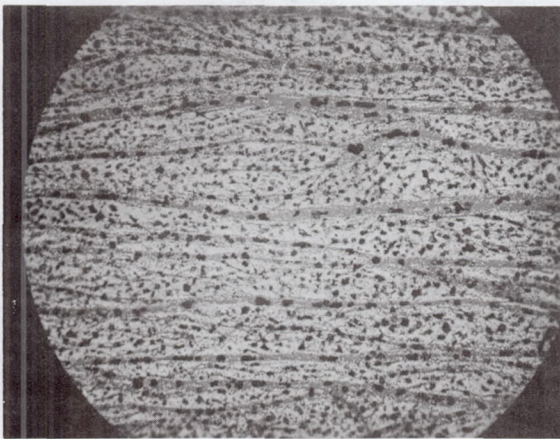




(a) 1.25 percent voids.



(b) 3.9 percent voids.



(c) 12.1 percent voids.

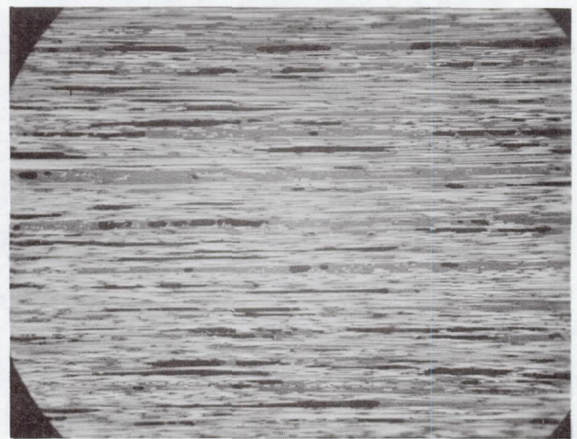
Figure 5.—Fiber-end views of composites.



(a) 1.25 percent voids.



(b) 3.9 percent voids.



(c) 12.1 percent voids.

Figure 6.—Fiber-side view of composites.



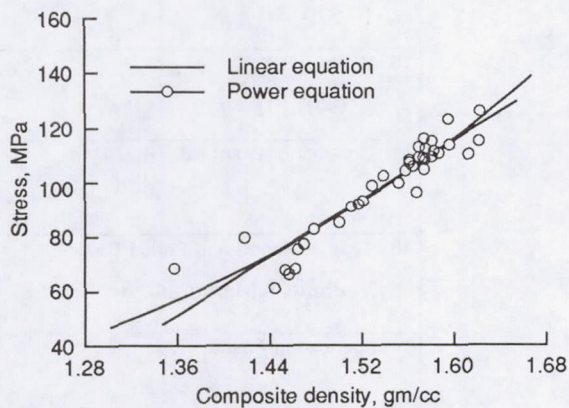


Figure 7.—AS4 graphite/PMR-15 ILSS as a function of composite density.

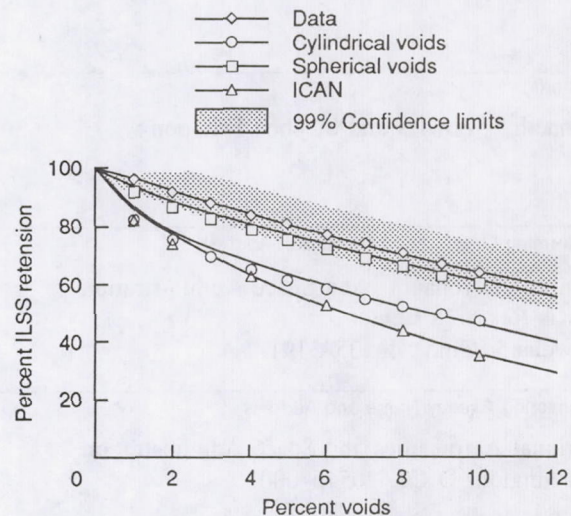


Figure 8.—Interlaminar shear strength as a function of void content for 60 percent fiber volume fraction of AS/PMR-15 unidirectional composites.

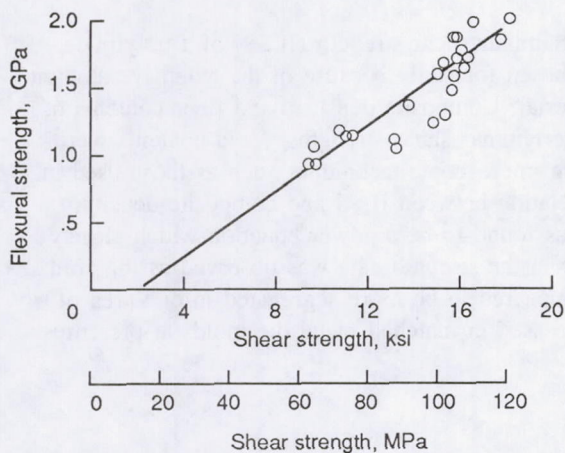


Figure 9.—The correlation of ILSS with flexural strength for AS/PMR-15 unidirectional composites.

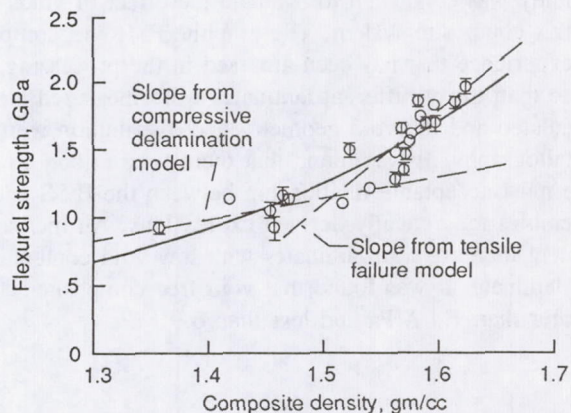


Figure 10.—Composite flexural strength as a function of composite density.



# Report Documentation Page

1. Report No. NASA TM-103267		2. Government Accession No.		3. Recipient's Catalog No.	
4. Title and Subtitle  A Study of Void Effects on the Interlaminar Shear Strength of Unidirectional Graphite Fiber Reinforced Composites				5. Report Date October 1990	
				6. Performing Organization Code	
7. Author(s)  Kenneth J. Bowles and Stephen Frimpong				8. Performing Organization Report No. E-5704	
				10. Work Unit No. 510-01-01	
9. Performing Organization Name and Address  National Aeronautics and Space Administration Lewis Research Center Cleveland, Ohio 44135-3191				11. Contract or Grant No.	
				13. Type of Report and Period Covered Technical Memorandum	
12. Sponsoring Agency Name and Address  National Aeronautics and Space Administration Washington, D.C. 20546-0001				14. Sponsoring Agency Code	
15. Supplementary Notes					
16. Abstract  A study was conducted to evaluate the effect of voids on the interlaminar shear strength (ILSS) of a polyimide matrix composite system. The graphite/PMR-15 composite was chosen for study because of the extensive amount of experience that has been amassed in the processing of this material. Composite densities and fiber contents of more than thirty different laminates were measured along with interlaminar shear strengths. Void contents were calculated and the void geometry and distribution were noted using microscopic techniques such as those used in metallography. It was found that there was a good empirical correlation between ILSS and composite density. The most acceptable relationship between the ILSS and density was found to be a power equation which closely resembles theoretically derived expressions. An increase in scatter in the strength data was observed as the void content increased. In laminates with low void content, the voids appeared to be more segregated in one area of the laminate. It was found that void free composites could be processed in matched metal die molds at pressures greater than 1.4 MPa and less than 6.9 MPa.					
17. Key Words (Suggested by Author(s))  Composites; Polymers; Fibers; Mechanical properties; Interlaminar shear strength; Void effects; Density			18. Distribution Statement  Unclassified - Unlimited Subject Category 34		
19. Security Classif. (of this report) Unclassified		20. Security Classif. (of this page) Unclassified		21. No. of pages 30	
				22. Price* A03	